



# Influence of Al<sub>2</sub>O<sub>3</sub> and TiO<sub>2</sub> nanofluid on hard turning performance

Ramanuj Kumar<sup>1</sup> · Ashok Kumar Sahoo<sup>1</sup> · Purna Chandra Mishra<sup>1</sup> · Rabin Kumar Das<sup>1</sup>

Received: 25 January 2019 / Accepted: 25 November 2019 / Published online: 18 December 2019  
© Springer-Verlag London Ltd., part of Springer Nature 2019

## Abstract

The current paper emphasized on preparation methodology of aqueous Al<sub>2</sub>O<sub>3</sub>-water and TiO<sub>2</sub>-water nanofluids and its application as the coolant in hard turning operations. The nanofluids are prepared through the two-step process, dispersing nanoparticles of Al<sub>2</sub>O<sub>3</sub> (average diameter 44 nm) and TiO<sub>2</sub> (average diameter 27 nm) in deionized water at three different % weight concentrations (0.005, 0.01, and 0.05). Air-assisted nanofluid is impinged through spray impingement setup in hard turning of AISI D2 steel (55 HRC) using multilayer (TiN/TiCN/Al<sub>2</sub>O<sub>3</sub>)-coated carbide tool. Application of nanofluid through spray impingement technique in hard turning is a novel work which is rarely found in the literature. Also, there is no literature available which presented the comparative hard turning performance under lower weight % concentration of Al<sub>2</sub>O<sub>3</sub> and TiO<sub>2</sub> nanofluid although the cost of the nanoparticle is high. Further, flank wear (V<sub>Bc</sub>), cutting temperature (T), average surface roughness (Ra), and chip morphology have been investigated as the cutting responses. Abrasion is the dominant wear mechanism identified for both types of nano cutting fluids. TiO<sub>2</sub>-water nanofluid attributes enhanced machinability compared with that of Al<sub>2</sub>O<sub>3</sub>-water nanofluid due to higher lubricious characteristics of TiO<sub>2</sub> which significantly reduces the chip-tool friction thus reduces the cutting heat. The most favorable results are noticed at 0.01% weight concentration of TiO<sub>2</sub> and at this condition, compared with the same concentration of Al<sub>2</sub>O<sub>3</sub> nanofluid, 29% reduction in tool-flank wear, 9.7% drop in cutting temperature, and 14.3% reduction in surface roughness are found. Tool life at 0.01 wt% concentrations of TiO<sub>2</sub> nanofluids is found to be 154 min taking flank wear criteria of 0.3 mm, which is 2.52 times more than the tool life obtained under dry cutting and 1.47 times higher than the tool life obtained under air-water spray impingement due to excellent wettability, lubrication, and heat dissipation capability of TiO<sub>2</sub> nanofluid. However, the employment of deionized water-based TiO<sub>2</sub> nanofluid in spray impingement cooling hard machining can be very promising for a practical manufacturing concern.

**Keywords** Nanoparticle · Nanofluid · Spray · Wear · Machinability · Temperature · Chip · Roughness

## 1 Introduction

A challenge in high-speed machining is the elevation of cutting temperature that leads to the reduction in tool life and surface deformities of a machined work specimen. Thus, the application of cutting fluid has come into existence to reduce the cutting temperature, chip-tool friction, and flushing out the chips from cutting zone during a machining operation. Apart from this, the function of the cutting fluid during hard machining is to promote economic feasibility of insert; retain tight

tolerances, reduction of thermal deformities of work-specimen, and retain the native properties of the machined surface [1]. Traditional cutting fluids (straight cut oil, soluble oil, semi-synthetic, and synthetic fluids) have outstanding lubricious characteristics but underprivileged thermal characteristics that confine the productivity of any machining process in the metal cutting industry. In the current scenario, a wide range of approaches is existing to improve the heat dissipating rate of coolant in machining. One such proven approach possibly may be the inclusion of miniature size (mm and μm) of the solid particle in the conventional cutting fluid which can improve its thermal characteristics. Utilization of these cutting fluids may reveal crucial issues like blockage/clogging, pressure fall in supply pipelines, high erosion, and underprivileged stability of the suspension. However, since recent decades, nano-sized particles substituted these milli/micro-sized particles in the fluid suspension and promoting the advancement of

✉ Ashok Kumar Sahoo  
aklala72@gmail.com

<sup>1</sup> School of Mechanical Engineering, Kalinga Institute of Industrial Technology (KIIT), Deemed to be University, Bhubaneswar-24, Odisha, India

a novel category of lubricant/fluid known as “nanofluids” or “nanolubricants.” These nanofluids have various favorable characteristics over conventional cutting fluids such as superior thermal conductivity, improved stability, minimal coagulation, and minor pressure drop in the supply system. The application of nanofluids has noticed a significant enhancement in the performance of input process parameters during various machining operation of hard to cut metals and their alloys [2]. In addition to thermal conductivity, the frictional force between tool work may be a significant factor regarding temperature elevation at the cutting zone, which also attributes to the dimensional deviation, poor finished surface quality, and reduced tool life. So, an addition of some self-lubricating nanoparticle (low frictional behavior) into the base fluid will increase the lubricious characteristics of regular coolants owing to the decline of the coefficient of frictions. Thus, these nanolubricants may help in the reduction of cutting temperature, tool wear, cutting force, and surface roughness during hard machining [3].

In recent years, lots of research articles illustrated the benefits of the application of different kinds of nanofluids in hard turning. Sidik et al. [4] reported the effective reduction in friction coefficients as well as in wear results; however, efficiency, as well as reliability of machining process and machining tools, was improved under nanofluid coolant relative to other coolants. Rapeti et al. [5] stated that the type of base liquid was the most vibrant input term which attributed the highest impact on cutting performances succeeded by nanoparticle concentration, cutting speed, and cutting feed. Singh et al. [6] proposed that the diameter of nanoparticle significantly affects the machining responses as leading the particle size reduced the force and surface roughness. Sharma et al. [7] found an effective enhancement in viscosity, density, and thermal conductivity of nano cutting fluid concerning the rise in the concentration of nanoparticles while specific heat was reduced. This facilitated the remarkable decline in wear, cutting force, and roughness of the machined surface in comparison with dry and mist machining. Hegab et al. [8] stated that the inclusion of nano powder into the base fluid successfully enhanced the enactment of MQL.

Some popularly used nanofluids are based on graphene, alumina ( $\text{Al}_2\text{O}_3$ ), silicon dioxide ( $\text{SiO}_2$ ), multi-walled carbon nanotubes (MWCNTs), molybdenum disulfide ( $\text{MoS}_2$ ), graphite, etc. All these nanofluids were mostly used in machining through minimum quantity lubrication (MQL) technique. Hybrid nanofluid (alumina/graphene) was used by Sharma et al. [9] and noticed the reduction in interface temperature and wear at the flank face by 5.79% and 12.29% respectively compared with alumina-enriched nanofluid. Also, the thermal coefficient and lubricating capabilities of nanofluid were increased with an increase in nanoparticle concentration in the base-machining fluid. Chetan et al. [10] reported the lower magnitudes of nose wear and flank wear in

machining with  $\text{Al}_2\text{O}_3$  nanofluid due to the formation of tribo layer compared with silver nanofluid and sunflower oil–mixed water cutting fluid. Khandekar et al. [11] noticed that with addition by volume of 0.01 concentration of  $\text{Al}_2\text{O}_3$  nanoparticles to the regular coolant, its wettability property was highly improved compared with regular fluid and natural water. Also, the enormous decrement in gradual wears (flank and crater wear) was identified due to favorable thermal properties, enhanced wettability, and the lubricating capability of the nanofluid. Minh et al. [12] concluded that the implementation of 0.5% volume concentration of  $\text{Al}_2\text{O}_3$  nanofluid through MQL may economical and advantageous for the milling process. The obtained surface integrity was enhanced and equivalent to grinding results. Sayuti et al. [13] utilized mineral oil–based silicon dioxide (5–10 nm size) nanofluid through MQL in hard turning of AISI 4140 steel and found preeminent flank wear and surface roughness at 0.5% weight concentration of nanofluid. Garcia et al. [14] stated that the concentration of nanoparticles ( $\leq 0.1\%$  in weight) attributed the significant change in the machining performance. At 0.055% weight concentration, surface quality enhanced by 69% compared with without added-cutting fluid. Kadirgama et al. [15] found the higher thermal conductivity of ethylene-glycol/nano-cellulose-based nanofluid when the volume concentration of nano-inclusion is 0.5%. Nanofluid with higher thermal conductivity worked as a heat transporter by carrying the majority of generated heat, thus delayed the tool wear and attributed the fine finish surface. Najiha et al. [16] observed micro-attrition, micro-abrasion, and adhesion types of wear mechanism during machining of aluminum alloy under MQL-assisted water-based  $\text{TiO}_2$  nanofluid. Water-based nanofluid is more favorable for edge integrity as chipping and fracture are dominant in the higher depth of cut conditions. 2.5% of the volume fraction of  $\text{TiO}_2$  nanofluid is highly feasible towards tool damage. Rahman et al. [17] prepared vegetable oil–based nanofluids by the inclusion of three different nanoparticles ( $\text{Al}_2\text{O}_3/\text{MoS}_2/\text{rutile-TiO}_2$ ) and carried an experimental investigation in turning of titanium alloy. Lowest concentration (0.5%) of  $\text{Al}_2\text{O}_3$ -canola nanofluid attributed the lowest surface roughness (0.248  $\mu\text{m}$ ) while at the same concentration,  $\text{MoS}_2$ -canola nanofluid attributed the lowest cutting temperature (875 °C).

According to Sahu et al. [18], carbon nanotube–dispersed cutting fluid application enables a noteworthy amount of reduction in wear at the flank surface, cutting force, and roughness of the turned surface in comparison with dry as well conventional fluid application in Ti-6Al-4V machining. Raju et al. [19] utilized nano size carbon tube–mixed cutting fluid in hard turning of EN31 grade steel and got enhanced results of forces and work surface finish relative to conventional coolants. Padmini et al. [20] found that the tool-tip wear, average roughness of the machined surface, cutting forces, and cutting temperature were diminished by 44%, 39%, 37%, and 21%

respectively using coconut-mixed nano molybdenum disulfide with 0.005 concentrated cutting fluid in correlation to machining under dry condition. Musavi et al. [21] compared the surface quality of superalloy under different cooling environment. MQL exhibits better results relative to flood cooling. Due to the spherical outline of CuO nanoparticle, CuO-based nanofluid attributes better lubrication capability relative to SiO<sub>2</sub>. Nanofluid with surfactant exhibits 14% less surface roughness relative to conventional fluid while un-added surfactant nanofluid exhibits 4% less surface roughness relative to the conventional fluid. Amrita et al. [22–24] emphasized on the comparative assessment of machining responses in turning operation of AISI 1040 grade steel under four different cooling surroundings like nano graphite soluble oil, soluble oil, flood lubrication, and dry. The enhanced performances were reported with the application of nano graphite-enriched soluble oil. In another work, nano molybdenum disulfide fluid provided improved wear properties and quality of finish, and reduced cutting forces compared with wet, dry, and functionalized nano graphite conditions. Surface quality got enhance with rising concentration of nano graphite in cutting fluid for both MQL processes. Su et al. [25] implemented two steps method to prepare graphite-dispersed nano cutting fluids. The properties, namely surface tension, viscosity, thermal conductivity, and wettability of nanofluids, have been calculated. Graphite-oil mixed nanofluid through MQL attributed the significant reduction in temperature as well as in cutting force relative to dry and regular MQL. Duc et al. [26] stated that the type of nanoparticle followed by base fluid was the most influencing agent to influence the surface roughness in MQL machining. Compared with MoS<sub>2</sub> nanofluid, Al<sub>2</sub>O<sub>3</sub> nanofluid attributed the better surface finish. Hegab and Kishawy [27] found better surface quality and power consumption in turning of Inconel 718 alloy under MWCNTs nanofluid compared with Al<sub>2</sub>O<sub>3</sub> nanofluid. Dong et al. [28] utilized three different weight % concentrations 0.2, 0.5, and 0.8 of MoS<sub>2</sub> through MQCL (minimum quantity cooling lubrication) technique in hard milling of tool steel and found better surface finish at 0.5 wt% concentration compared with dry, MQL, and pure fluid-assisted MQCL.

Based on the literature study, the application of nano Al<sub>2</sub>O<sub>3</sub> and nano TiO<sub>2</sub> suspension cutting fluid in hard turning application is inadequate and has not been studied so far under the spray impingement technique. However, this novelty of work definitely helps the researchers to carry further research using different base fluids in hard turning. The objective of the present study is as follows:

- To synthesize the Al<sub>2</sub>O<sub>3</sub> and TiO<sub>2</sub> nanoparticles using high-speed ball mill and prepared the deionized water-based Al<sub>2</sub>O<sub>3</sub> and TiO<sub>2</sub> nanofluid.
- Comparative analysis of machining performance under Al<sub>2</sub>O<sub>3</sub>-water- and TiO<sub>2</sub>-water-based nanofluid using spray

impingement technique during turning of heat-treated AISI D2 steel.

- Tool life evaluation under best nanofluid concentration.

## 2 Materials and methods

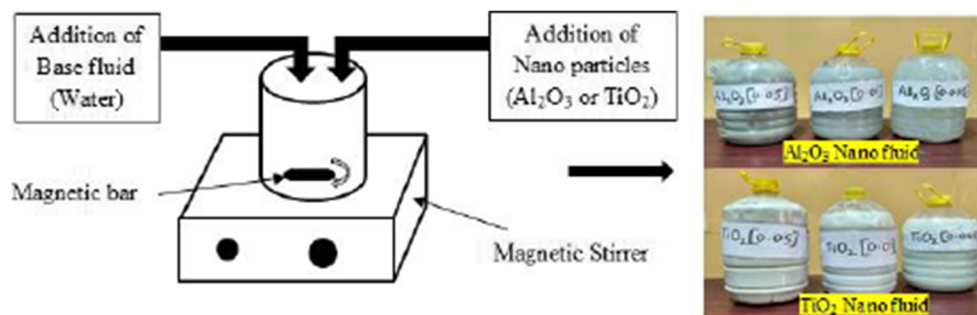
Commercially available Al<sub>2</sub>O<sub>3</sub> and TiO<sub>2</sub> micro-sized powders (99.8% purity with an approximate size of 45 μm) are collected and processed through a high-energy ball mill to prepare the nanoparticles. The milling operation is performed for a period of 10 h with a milling speed of 300 rpm. For every 1 h, the ball mill has been kept in off mode for 30 min to cool down the machine. The following steps have been used for the preparation of nanoparticles [29]:

- Step 1: Placement of ball and powder inside the hardened steel jar with 10:1 hardened steel ball to powder ratio (360 g weight of balls and 36 g weight of powder in a jar).
- Step 2: Addition of toluene in ball-powder-filled jar to make its paste for proper mixing.
- Step 3: Placement of jar into the ball mill and start milling with a speed of 300 rpm.
- Step 4: After completion of 10 h, the ball from the jar has been removed and put the paste material into a pan and left it till dry.
- Step 5: Last step involved to break it into fine sizes.

Further characterization of nanoparticles and preparations of nanofluids using two-step concepts (Fig. 1) are discussed as follows:

The elemental composition of nanoparticle has been verified using EDS (energy dispersive spectroscopy) analysis in Fig. 2 a and b and it confirms the presence of associated elements in Al<sub>2</sub>O<sub>3</sub> and in TiO<sub>2</sub> nanopowders. Particle size measurement has been carried by field emission scanning electron microscopy (FESEM) image as displayed in Fig. 2 c and d. The particle size distribution for both particles is displayed in Fig. 2 e and f and the size for Al<sub>2</sub>O<sub>3</sub> powder and TiO<sub>2</sub> powder are found to be in a range of 30–60 nm (average size 44 nm) and 15–35 nm (average size 27 nm), respectively. Clustering of the nano Al<sub>2</sub>O<sub>3</sub> particles is clearly visible in Fig. 2c. However, the size of the nano Al<sub>2</sub>O<sub>3</sub> particle is relatively more to nano TiO<sub>2</sub> particle. In the available literatures, the size of nanoparticles mostly found to be less than 100 nm [1, 6, 21]. The particle size distribution of nanofluids was estimated by DLS (dynamic light scattering) method with Zetasizer instrument (Malvern make) which works on the tyndall scattering of nanoparticles in base fluids. Average particle distribution (hydrodynamic diameter) for Al<sub>2</sub>O<sub>3</sub> particle is found to be about 1538 nm, Fig. 2g, and similarly for TiO<sub>2</sub>,

**Fig. 1** Preparation of deionized water-based  $\text{Al}_2\text{O}_3$  and  $\text{TiO}_2$  nanofluids



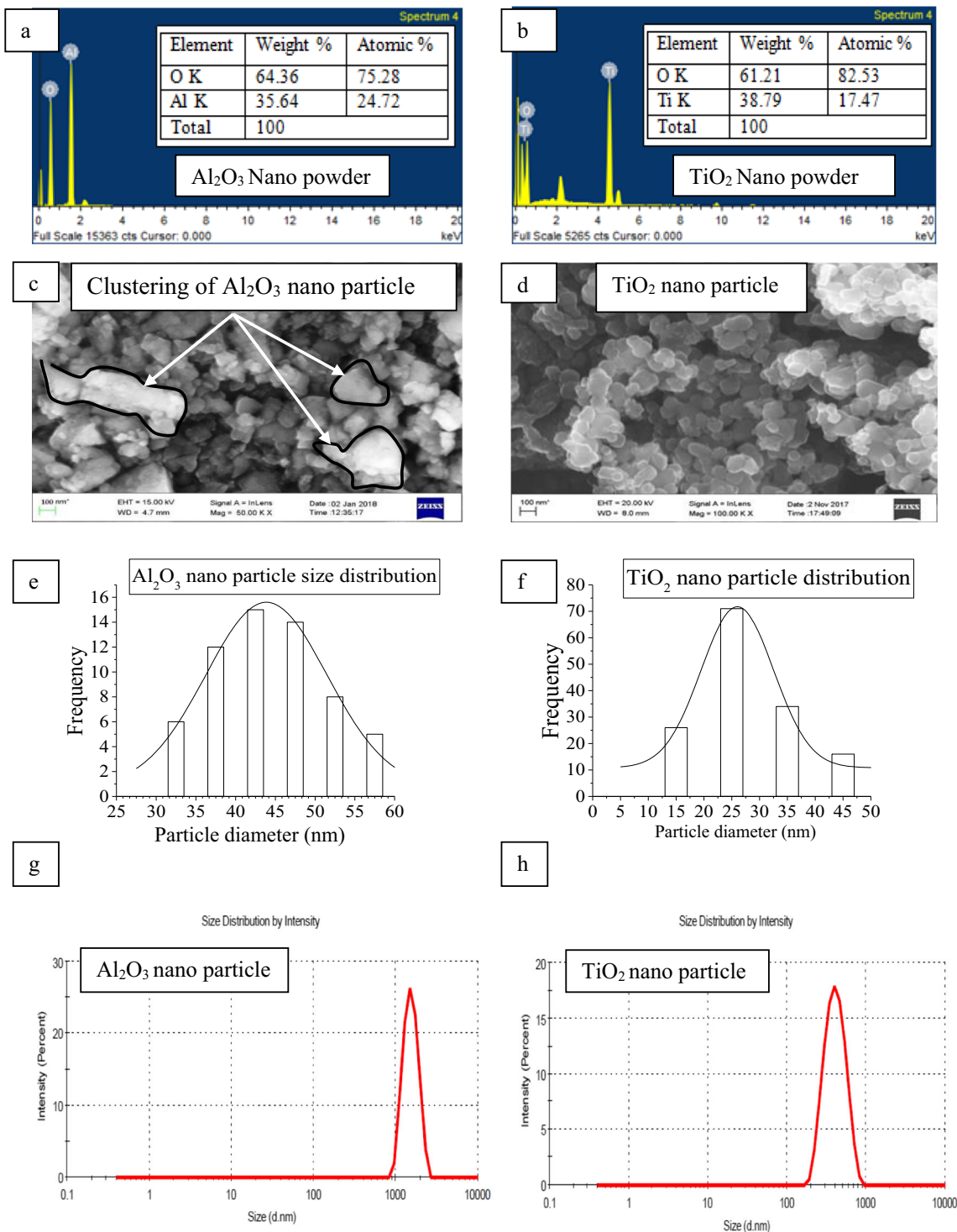
it is noticed to be about 417.8 nm, Fig. 2h. Karimzadehkhoei et al. [30] also carried the DLS analysis of  $\text{TiO}_2$  particle and found the hydro-dynamic diameter in between 300 to 380 nm. At room temperature (25 °C), the thermal conductivity of  $\text{Al}_2\text{O}_3$  and  $\text{TiO}_2$  nanopowders are calculated as  $34 \text{ Wm}^{-1} \text{ K}^{-1}$  and  $11.7 \text{ Wm}^{-1} \text{ K}^{-1}$ , respectively [29]. The thermal conductivity and viscosity of the base fluid (deionized water) at room temperature (25 °C) is found as  $0.607 \text{ Wm}^{-1} \text{ K}^{-1}$  and  $0.89 \text{ mPa.s}$  [31]. The density of  $\text{Al}_2\text{O}_3$ ,  $\text{TiO}_2$ , and deionized water are found as  $3970 \text{ Kg/m}^3$ ,  $4230 \text{ Kg/m}^3$ , and  $997 \text{ Kg/m}^3$ , respectively [29].

Nanofluids are prepared using a two-step methodology [25, 29], dispersing nano  $\text{Al}_2\text{O}_3$  and nano  $\text{TiO}_2$  particles into the base liquid (deionized water) with a steady magnetic stirring speed of 1000 rpm for the duration of 24 h. Three distinct weight concentrations (0.005%, 0.01%, and 0.05%) of nanofluid are prepared. Use of surfactant was completely prohibited during the preparation of nanofluids, since adding of any surfactant will lead to alteration to the property of nanofluid and corrosive to the cutting surface. However, after a 24-h mixing period, nanofluid is kept in a bottle to check its stability. For highest weight concentration (0.05%), the stability of both fluids is noticed to be about 5 days and beyond this, the phenomenon of clustering of nanoparticles started which leads to sedimentation in the base fluid. To maintain the stability or to break down the particle cluster, again magnetic stirring is applied for 4–5 h. Likewise, for both types of nanofluids, the stability of 0.01% and 0.005% weight concentration nanofluids are noticed as 9 and 13 days respectively and after this, stirring is applied for 4–5 h to get the stable solution [29]. Also, to verify the stability, UV-Vis Spectrophotometer (Orion Aqua Mate 8000 UV-Vis) is utilized to study the stability of each category of nanofluid. UV spectrophotometer test is a popular method to estimate the nanoparticle dispersion in terms of colloidal stability [32–33]. UV absorbance result of deionized water-based  $\text{Al}_2\text{O}_3$  and  $\text{TiO}_2$  nanofluid of different concentrations (0.005, 0.01, and 0.05 wt%) is displayed in Fig. 3 a and b, respectively. The absorbance of nanofluid lies in between 200 and 900 nm wavelengths. From Fig. 3, the absorbance of  $\text{Al}_2\text{O}_3$  is higher than  $\text{TiO}_2$ , i.e., more agglomerated nanoparticles are

present in  $\text{Al}_2\text{O}_3$  nanofluid compared with  $\text{TiO}_2$  nanofluid and it is also confirmed through FESEM image of both nanopowders (Fig. 2c, d). Due to this agglomeration of nanoparticles, tribological performance of  $\text{Al}_2\text{O}_3$  nanofluid will be less compared with  $\text{TiO}_2$  nanofluid. This graphical view (Fig. 3) reflects the characteristics of suspended nanoparticles and that increases with increasing weight % concentration of nanofluids. Hence, the stability of nanoparticle is decreasing with % weight concentration. Also, from this analysis, it can be said that the stability of nanofluid colloidal is maintained at each % weight concentration of both nanofluids.

Further, the thermal conductivity of nanofluids is measured at room temperature (25 °C) using thermal conductivity interferometer apparatus (Mittal Enterprise, Delhi, India). The thermal conductivity results are reported in Table 1. From Table 1, thermal conductivity for both nanofluids is increasing with weight % concentration of nano particles. For each concentration,  $\text{Al}_2\text{O}_3$  nanofluid has higher thermal conductivity compared with  $\text{TiO}_2$  nanofluid due to the higher thermal conductivity of  $\text{Al}_2\text{O}_3$  powder compared with  $\text{TiO}_2$  powder. The thermal conductivity of  $\text{Al}_2\text{O}_3$  nanofluid at weight % concentrations 0.005, 0.01, and 0.05 is improved by 0.065%, 0.131%, and 0.692% respectively from base fluid. Similarly, for  $\text{TiO}_2$  nanofluid at weight % concentrations 0.005, 0.01, and 0.05, the thermal conductivity is improved by 0.016%, 0.049%, and 0.21% respectively from the base fluid. Overall, for both fluids, the improvement in thermal conductivity is very less (<1%). The viscosity of nanofluid is calculated using Eq. 1 [34], where  $\mu_{nf}$  denotes the viscosity of nanofluid,  $\mu_{bf}$  represents viscosity of the base fluid, and  $\phi$  is volume fraction. According to Einstein, Eq. 1 is valid for viscous fluid having very low volume fraction ( $\phi$  less than 0.02) of spherical shaped particles [34]. The similar equivalent volume fraction is used in the current work; therefore, this relation is used to estimate the viscosity of nanofluid. For both nanofluids, viscosity is increasing with the particle concentration but improvement in viscosity is very less. Compared with base fluid, the maximum increment in viscosity of  $\text{Al}_2\text{O}_3$  nanofluid is 0.031% at the highest concentration (0.05 wt) while for  $\text{TiO}_2$  nanofluid, the maximum improvement in viscosity is 0.029% at higher concentration, i.e., very less



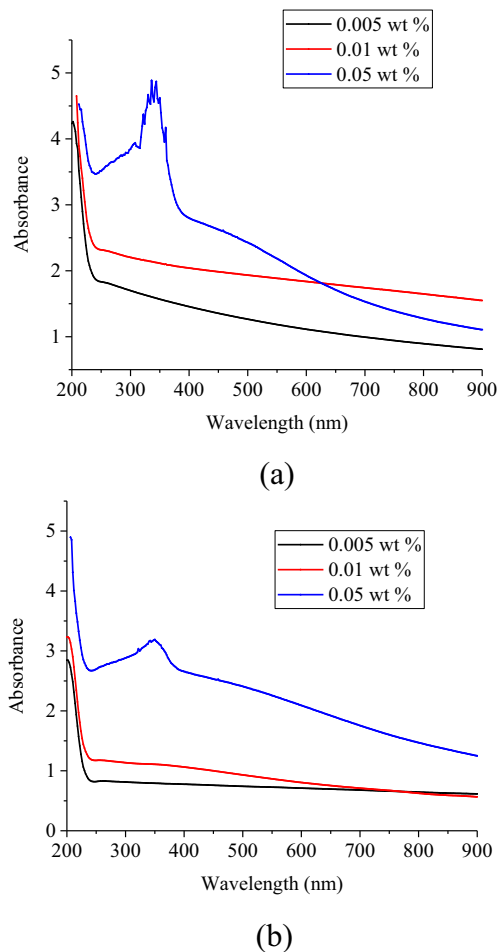


**Fig. 2** a, b EDS view for nanopowders. c, d FESEM micrographs of nano particles. e, f Particle size distribution of nanopowders. g, h DLS for distribution of nanoparticles in base fluid

improvement in viscosity has been observed with addition of nanoparticles in the deionized water. Density for each nanofluid is measured and reported in Table 1. From density results, nanofluid density increases with the concentration of nanoparticle in the base fluid. Density is also very less altered with addition of the low amount of nano particles, as

maximum improvement in density for Al<sub>2</sub>O<sub>3</sub> and TiO<sub>2</sub> nanofluid is noticed as 0.037% and 0.038% at the highest concentration (0.05% weight), respectively.

$$\mu_{nf} = (1 + 2.5\phi)\mu_{bf} \tag{1}$$



**Fig. 3** UV spectrophotometer absorbance result for water-based **a**  $\text{Al}_2\text{O}_3$  nanofluid and **b**  $\text{TiO}_2$  nanofluid

HMT lathe has been utilized for turning experiments for hardened AISI D2 steel ( $55 \pm 1$ ) HRC specimen of diameter 48 mm and cutting length 200 mm at fixed cutting condition (cutting speed ( $v$ ) = 108 m/min, feed ( $f$ ) = 0.04 mm/revolution, depth of cut ( $d$ ) = 0.1 mm) [35–36] with multi-layered (TiN/TiAlN/ $\text{Al}_2\text{O}_3$ )-coated carbide insert (TN5120) of rhombus shape with ISO code CNMG 120408-22. The geometry associated with cutting insert is as follows: included angle  $80^\circ$ , approach angle  $95^\circ$ , rake angle  $-6^\circ$ , clearance angle  $5^\circ$ , nose radius 0.8 mm, and inbuilt chip breaker. The experimentations

have been accomplished under the spray impingement nanofluid cooling (SIC) scenario with air pressure ( $A_p$ ) 1.5 bar and nanofluid pressure ( $N_p$ ) 1 bar [36–38]. SIC setup has two inlets; the first inlet is air compressor and other inlet is the nanofluid tank. The nanofluid tank is attached with stirring motor (Fig. 4), which is rotated at 1000 rpm during experimentation. The nanofluid tank is placed on 15 m height from the base and allows the nanofluid into SIC setup due to gravity. The pressure of air and nanofluid is controlled by the pressure regulator knob. The nozzle has two inlet valves which are connected through air and nanofluid tube separately as shown in Fig. 4. The detail specification of spray impingement cooling (SIC) system and nozzle are given in Table 2. The flow rate of the spray cooling system depends on air and fluid pressure. The flow rate capacity of SIC system varies from 40 to 300 l per hour. In the present work, the flow rate of nanofluid at 1.5 bar air pressure and 1 bar nanofluid pressure is 60 l per hour. The straight  $\frac{1}{4}$  J pressure sprays internal mix nozzle is utilized for spraying the coolant. The shape of the spray is full cone round shape with cone angle varies from  $19^\circ$  to  $22^\circ$  and the current experimentation spray cone angle is measured as  $20^\circ$ . The distance between nozzle output and the cutting zone (tool-workpiece interface) is kept fixed at  $17 \pm 1$  cm. During spraying, full face of the tool-rake surface is covered which helps to discharge the chips from tool-rake face easily. Two different categories of nanofluids ( $\text{Al}_2\text{O}_3$  and  $\text{TiO}_2$ ) with three concentrations (0.005%, 0.01%, and 0.05% by weight) have been implemented as a coolant to study flank wear at nose corner called nose wear (VBc), surface roughness ( $R_a$ ), cutting temperature ( $T$ ), and chip morphology. Each experiment has been repeated three times and the mean value of each response has been noted down. The failure criteria for  $\text{VBc} = 0.3$  mm and  $R_a = 1.6$   $\mu\text{m}$  have been selected [35–36, 38, 39]. The width of flank wear at tool nose has been measured using Olympus made STM 6 optical microscope with stream basic software at  $\times 50$  magnification.  $R_a$  has been measured using Taylor Hobson precision surface finish tester where stylus evaluation length is 4 mm and Gauss length is 0.8 mm.  $T$  (cutting temperature) is measured with FLUKE made Ti32 infrared thermal camera with 0.81 emissivity [40]. Chip morphology has been discussed on the basis of chip image captured by an optical microscope with  $\times 30$

**Table 1** Thermal conductivity, viscosity, and density results of nanofluids

Weight % concentration	Thermal conductivity ( $\text{Wm}^{-1} \text{K}^{-1}$ )		Viscosity (mPa.s)		Density ( $\text{Kg/m}^3$ )	
	$\text{Al}_2\text{O}_3$	$\text{TiO}_2$	$\text{Al}_2\text{O}_3$	$\text{TiO}_2$	$\text{Al}_2\text{O}_3$	$\text{TiO}_2$
0.005	0.6074	0.6071	0.890028	0.890026	997.037	997.038
0.01	0.6078	0.6073	0.890056	0.890053	997.074	997.077
0.05	0.6112	0.6083	0.890279	0.890266	997.373	997.387

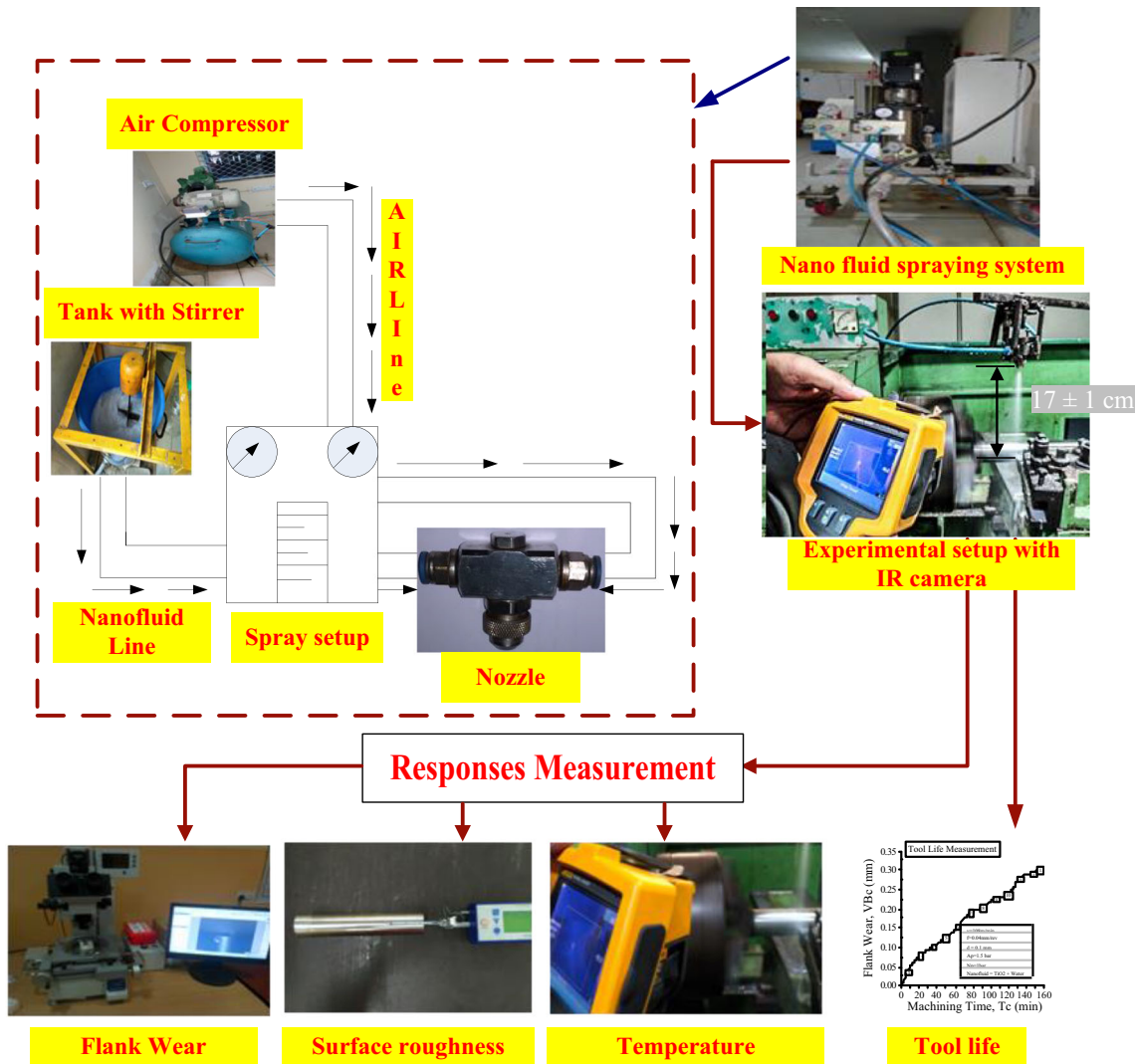


Fig. 4 Pictorial details of hard turning experiment

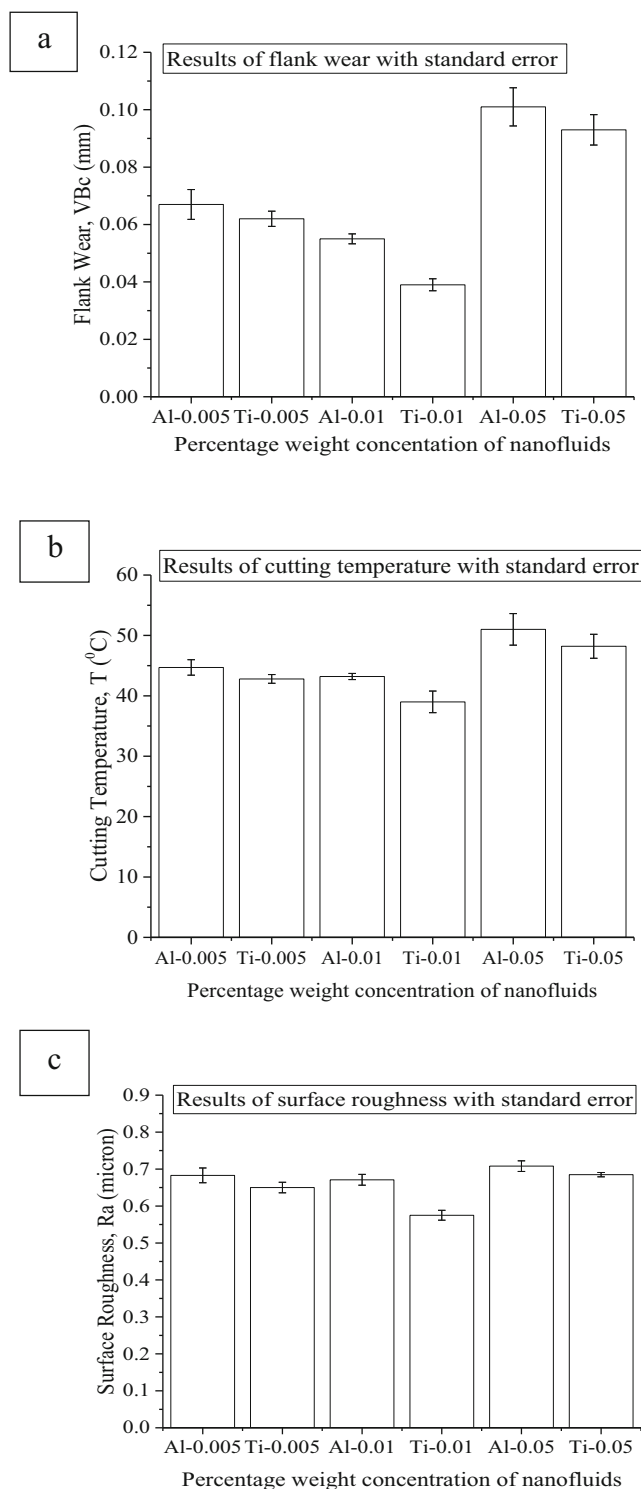
magnification. The pictorial display of experimental details has been shown in Fig. 4.

Table 2 Details of spray impingement cooling setup

Spray Impingement cooling setup	Spraying System Pvt. Ltd. (India)
Nozzle specification	Type: Straight ¼ J spray mix Diameter = 10 mm Shape of spray pattern: full cone round shape Spray cone angle = 19 to 22° Continuous spray distance = up to 120 cm
Nozzle to cutting zone perpendicular distance	17 ± 1 cm
Flow rate of pump	2.5 m <sup>3</sup> /h
Maximum head of pump	56 m
Air compressor	Up to 6 bar
Flow rate spray	40 to 300 l per hour

### 3 Results and discussion

The experimental results data of flank wear are reported in Figs. 5a and 6. Among all tests, nano TiO<sub>2</sub> cutting fluid (0.01% weight concentration) exhibits the lowest flank wear of 0.039 mm. At the same cutting parameters, flank wear was found to be 0.055 mm under dry condition [35] and 0.054 mm under air-water mist spray impingement cooling [36]. This yields about 29% less tool wear using nano TiO<sub>2</sub> fluid (0.01% weight) compared with dry cutting. Similarly, 27.7% less tool wear is noticed in nano TiO<sub>2</sub> fluid (0.01% weight) compared with air-water-based spray impingement cooling. It may happen due to better wettability characteristics of nano TiO<sub>2</sub> fluid which enhances the lubricating and heat removal properties during machining. Also, in nano fluid spray cooling, the nanoparticles are separated by the higher velocity air and revolve between tool-workpiece interfaces and create a favorable rolling effect. Due to this rolling effect, the contact area between chip and tool reduces thus lower heat generated



**Fig. 5** Experimental results of **a** VBc, **b** T, and **c** Ra

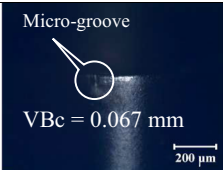

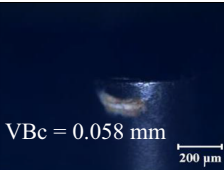

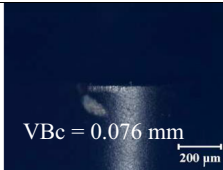

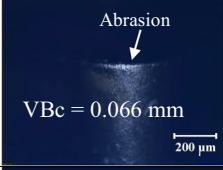

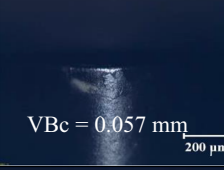
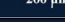
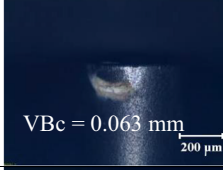

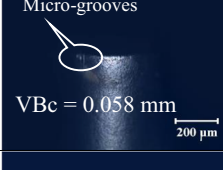



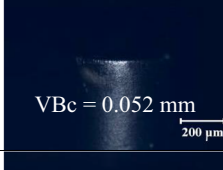

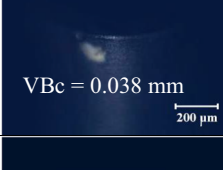

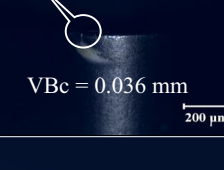

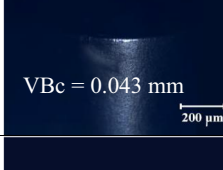

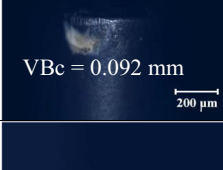

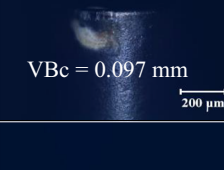

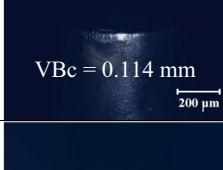

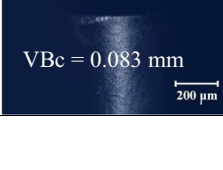

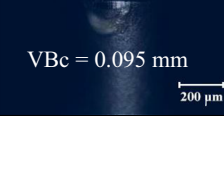

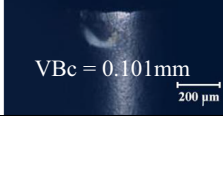

and delayed the wear rate [21, 41]. From the wear results of both nanofluids (Fig. 6), at the lowest concentration (0.005 wt%), the tool-wear is higher compared with 0.01 wt% concentration due to less number of nanoparticles present in water which retard the capability of nanofluid to reduce the friction coefficient [42]. Further on the highest

concentration (0.05%), tool wear is highest for both nanofluids. Higher nanoparticle concentration leads to nano-additives wear which undesirably affects the tool wear; thus, in the current work, tool wear is highest at the highest nanofluid concentration of each nanofluid [26, 43]. In every set of concentrations, nano TiO<sub>2</sub> coolant performs superior to nano Al<sub>2</sub>O<sub>3</sub> coolant even if thermal conductivity Al<sub>2</sub>O<sub>3</sub>-based coolants have little more thermal conductivity. Therefore, wear results show that the self-lubricating phenomena of TiO<sub>2</sub> are more dominant over thermal conductivity which leads to lessening in tool-flank wear growth under TiO<sub>2</sub> coolant compared with Al<sub>2</sub>O<sub>3</sub> coolant. In the spraying process, nanofluid gets atomized to very fine droplets which strike on work as well as tool surface. As a result, tribological properties significantly improved which reduces the friction at cutting zone and lowers the tool wear [44]. From the FESEM image, Fig. 2c, it can be easily identified that the clustering phenomena are more dominant in nano Al<sub>2</sub>O<sub>3</sub> particles relative to nano TiO<sub>2</sub>. However, TiO<sub>2</sub> exhibits more lubricious effects and reduces the chip-tool friction more significantly by retaining tool hardness and stability for a longer duration for reduction of wear compared with nano Al<sub>2</sub>O<sub>3</sub> cutting fluid. Additionally, according to Khajezadeh et al. [45], flank wear width was improving with increasing the size of nanoparticle. In the current work, the average particle size of Al<sub>2</sub>O<sub>3</sub> nano powder is 63% higher than the TiO<sub>2</sub> nanopowder; therefore, the flank wear growth under TiO<sub>2</sub> nanofluid is less compared with Al<sub>2</sub>O<sub>3</sub> nanofluid. Further, from UV-Vsi Spectrophotometer results (Fig. 3a, b), TiO<sub>2</sub> nanofluid is more stable than Al<sub>2</sub>O<sub>3</sub> nanofluid; thus, more wear is noticed under Al<sub>2</sub>O<sub>3</sub>-based coolant. From wear micrographs (Fig. 6), abrasion is most dominant in each run and micro-grooves are also identified in machining under lower concentrations of nanofluid [46]. Abrasion phenomena during cutting occur due to hard element like chromium is present on the underside of the chip, which passes over the tool face continuously and removes the tool coating material by mechanical action [47]. Micro-grooves are developed due to hard particle chromium comes in contact with relatively softer material of tool [48]. Adhesion is not identified in any runs because of nano cutting coolant has better lubrication and wettability characteristics [44, 49].

From Fig. 7, the cutting temperature of the cutting zone first decreased and then increased with increasing nanofluid concentration. Lower concentration nanofluid (0.005 wt%) has less thermal conductivity as a result heat transfer rate is lower compared with other higher concentration nano fluid as a result cutting temperature is higher in low concentration nanofluid. Further, at the medium concentration (0.01 wt%), thermal conductivity improved that is why heat transfer rate increases thus cutting temperature reduces. But at highest concentration (0.05 wt%), although the thermal conductivity of nanofluid increases, heat transfer rate increases but due to higher number of nanoparticles present in the fluid, the



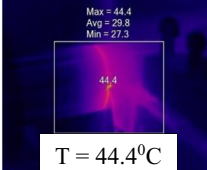
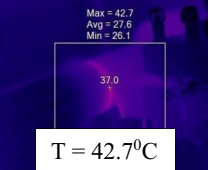
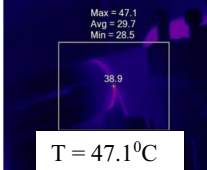
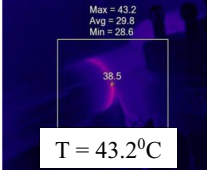
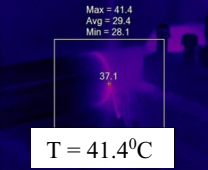
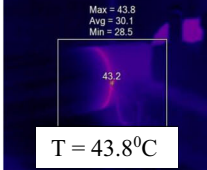
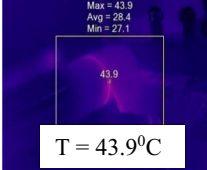
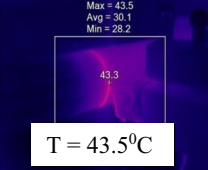
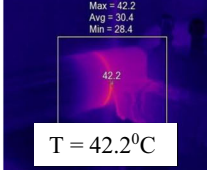
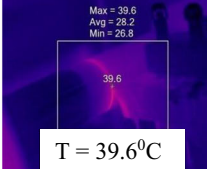
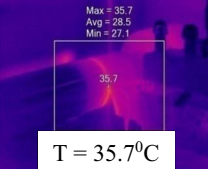
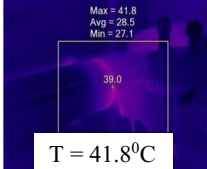
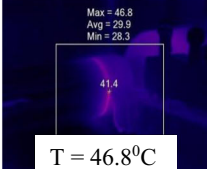
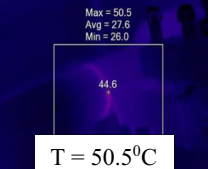
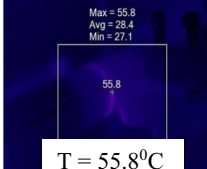
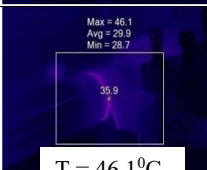
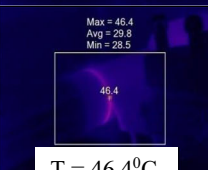
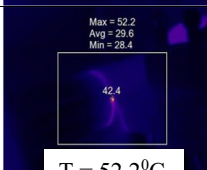
**Fig. 6** Experimental results of nose flank wear

Types of Nano fluids	Test run-1 VBc	Test run-2 VBc	Test run-3 VBc	Average VBc
Al <sub>2</sub> O <sub>3</sub> 0.005 %weight concentration	 Micro-groove VBc = 0.067 mm 	 VBc = 0.058 mm 	 VBc = 0.076 mm 	0.067 mm
TiO <sub>2</sub> 0.005 %weight concentration	 Abrasion VBc = 0.066 mm 	 VBc = 0.057 mm 	 VBc = 0.063 mm 	0.062 mm
Al <sub>2</sub> O <sub>3</sub> 0.01 %weight concentration	 Micro-grooves VBc = 0.058 mm 	 Micro-groove VBc = 0.055 mm 	 VBc = 0.052 mm 	0.055 mm
TiO <sub>2</sub> 0.01 %weight Concentration	 VBc = 0.038 mm 	 Micro-groove VBc = 0.036 mm 	 VBc = 0.043 mm 	0.039 mm
Al <sub>2</sub> O <sub>3</sub> 0.05 % weight Concentration	 VBc = 0.092 mm 	 VBc = 0.097 mm 	 VBc = 0.114 mm 	0.101 mm
TiO <sub>2</sub> 0.05 %weight Concentration	 VBc = 0.083 mm 	 VBc = 0.095 mm 	 VBc = 0.101mm 	0.093 mm

friction or shearing or collision phenomena in between nanoparticles is dominant and produces additional heat; as a result, cutting temperature at highest concentration is highest among all concentration nanofluid. According to Xuan and Li [50], the improvement in thermal conductivity is also depending on the interaction and collision among nanoparticles in the base fluid. Fathima and Mujeeb [51] stated that the thermal transportation of nanofluid can be attributed through collision among nanoparticles in the base fluid, the collision between the nanoparticle and base fluid and nano-convection phenomena in nanofluids. They stated that with increasing concentration up to a particular level, the base liquid layer (around the nanoparticle) effectively diffuse heat as the contact surface area increases. Hegab et al. [43] stated that the higher concentration leads to nano additive wear which enhances the tool wear; thus, higher temperature is found at a higher concentration of nanofluid. Also, during machining, a layer of nanoparticle is formed on to the tool tip and its thickness increases

with nanoparticle concentration, as sedimentation of nanoparticle on tool tip increase with the number of nanoparticle present in a nanofluid. Therefore, at a low level of concentration, sedimentation phenomena are less; however, layer thickness is less; thus, heat transfer as a result higher cutting temperature is found. Similarly, at the medium level, the thickness of formed layer is improved; as a result, the cutting temperature is reduced. But at the higher level, the layer thickness is more which creates a negative effect as it works as thermal resistance; thus, the cutting temperature is highest at tool tip. Higher layer thickness restricts the heat to dissipate; thus, this layer works as a thermal resistance layer which attributed the higher cutting temperature. Also, according to Das et al. [52], heat transfer of fluid is directly influenced by the viscosity of a fluid. Lager viscous fluid attributed the higher boundary thickness which reduces the convective heat transfer capability of fluid. In the current work, the viscosity of nanofluid at higher concentration is more; thus, boundary layer thickness is

**Fig. 7** Experimental results of cutting temperature

Types of Nano fluids	Test run-1 T	Test run-2 T	Test run-3 T	Average T
Al <sub>2</sub> O <sub>3</sub> 0.005 % weight concentration	 T = 44.4 <sup>0</sup> C	 T = 42.7 <sup>0</sup> C	 T = 47.1 <sup>0</sup> C	44.7 <sup>0</sup> C
TiO <sub>2</sub> 0.005 %weight concentration	 T = 43.2 <sup>0</sup> C	 T = 41.4 <sup>0</sup> C	 T = 43.8 <sup>0</sup> C	42.8 <sup>0</sup> C
Al <sub>2</sub> O <sub>3</sub> 0.01 %weight concentration	 T = 43.9 <sup>0</sup> C	 T = 43.5 <sup>0</sup> C	 T = 42.2 <sup>0</sup> C	43.2 <sup>0</sup> C
TiO <sub>2</sub> 0.01 % weight concentration	 T = 39.6 <sup>0</sup> C	 T = 35.7 <sup>0</sup> C	 T = 41.8 <sup>0</sup> C	39.0 <sup>0</sup> C
Al <sub>2</sub> O <sub>3</sub> 0.05 %weight concentration	 T = 46.8 <sup>0</sup> C	 T = 50.5 <sup>0</sup> C	 T = 55.8 <sup>0</sup> C	51.0 <sup>0</sup> C
TiO <sub>2</sub> 0.05 %weight concentration	 T = 46.1 <sup>0</sup> C	 T = 46.4 <sup>0</sup> C	 T = 52.2 <sup>0</sup> C	48.2 <sup>0</sup> C

higher; as a result, heat dissipation phenomena retard and it is confirmed through the cutting temperature results as the temperature is larger at higher concentrations. Further, cutting temperature (T) as revealed in Figs. 5b and 7 is found to be very low as compared with the temperature obtained by Kumar et al. [35] under dry cutting. Maximum average temperature (51 °C) obtained at the highest concentration (0.05%) of nano Al<sub>2</sub>O<sub>3</sub> cutting fluid is about 70% lower than the temperature obtained under the dry condition at same cutting and tooling conditions [35]. It may be due to improved tribological attributes, i.e., greater thermal conductivity as well as higher heat transfer characteristics of nanofluids [11, 53–54]. Further, it can be said that under spray impingement cooling, the movement of nanofluid particles are slower because of the resistance offered by air molecules; however, it separated the nanofluid into tiny ones thus easily penetrating around the

cutting zone and dissipated the cutting zone heat easily; thus, the cutting temperature has been lowered [41]. In every concentration, temperature obtained with nano TiO<sub>2</sub> cutting fluid is lower than that of temperature obtained under nano Al<sub>2</sub>O<sub>3</sub> cutting fluid due to self-lubrication properties and higher stability of TiO<sub>2</sub> nanofluid which dominated the favorable effect of higher thermal conductivity of Al<sub>2</sub>O<sub>3</sub> nanofluid. FESEM image, Fig. 2 c and d, also confirms the higher agglomeration of nano Al<sub>2</sub>O<sub>3</sub> particles relative to TiO<sub>2</sub> particles which reduces the favorable thermal behavior of Al<sub>2</sub>O<sub>3</sub> cutting fluid. As a result, a heat dissipation phenomenon reduces and attributes relatively higher cutting temperature. Among all set of experiments, lowest temperature obtained under nano TiO<sub>2</sub> cutting fluid (0.01% weight concentration) is with the average value of 39.0 °C which is 77.2% lower than the temperature (171 °C) obtained in dry condition with same turning

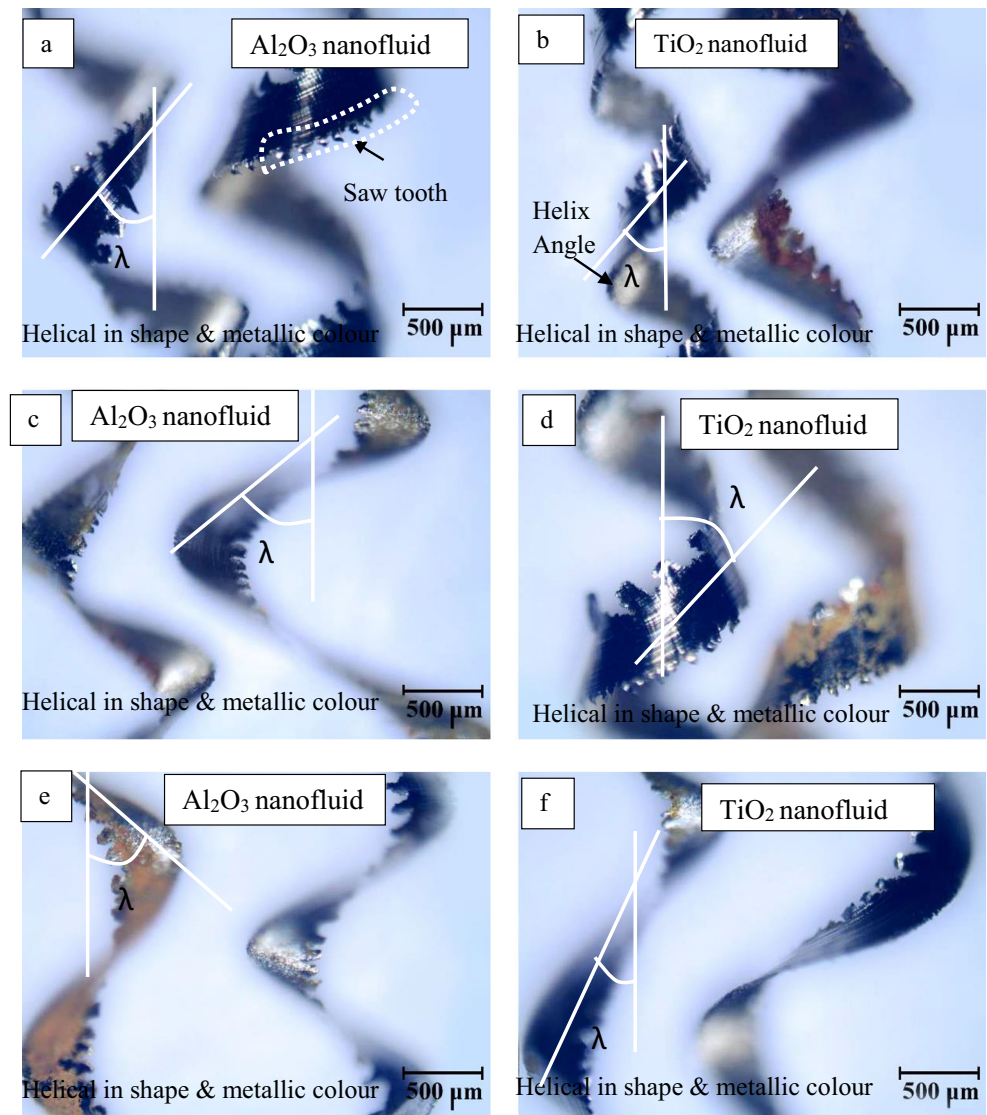
conditions [35]. Compared with air-water mist spray cooling [36], TiO<sub>2</sub> nanofluid produced 68.5% lower temperature due to the favorable rolling effect of nanofluid during cutting. Also at 0.01% weight concentration, TiO<sub>2</sub> nanofluid exhibits 9.72% lower magnitude of temperature compared with Al<sub>2</sub>O<sub>3</sub> due to higher wettability, greater lubricious, and higher stability of TiO<sub>2</sub> dispersed nanofluid found from UV-Vsi Spectrophotometer test results (Fig. 3a, b).

From the results, Fig. 5c, TiO<sub>2</sub> nanofluid provides lower surface roughness relative to Al<sub>2</sub>O<sub>3</sub> nanofluid. From the entire test results, nano TiO<sub>2</sub> cutting fluid (0.01% weight concentration) exhibits lowest surface roughness and provides about 14.3% lower roughness compared with nano Al<sub>2</sub>O<sub>3</sub> cutting fluid at the same concentration and about 11.5% lower surface roughness compared with dry condition at same cutting parameters [35]. From the FESEM image of both nano particles, Fig. 2c and d, the shape of particle is spherical but the shape and size of TiO<sub>2</sub> nanoparticle is more symmetric or more spherical compared with Al<sub>2</sub>O<sub>3</sub> nanoparticles; thus rolling effect is more dominating under TiO<sub>2</sub> nanofluid which led to enhanced lubrication effects compared with Al<sub>2</sub>O<sub>3</sub> nanofluid even if thermal conductivity of Al<sub>2</sub>O<sub>3</sub> nano fluid is minutely higher than TiO<sub>2</sub> nanofluid. Due to this, surface roughness is lower with TiO<sub>2</sub> nanofluid compared with Al<sub>2</sub>O<sub>3</sub> nanofluid. Additionally, finer size of TiO<sub>2</sub> nanoparticles easily penetrated into the tiny holes or scratches available on to the workpiece and tool (due to manufacturing defects) and therefore provided a uniformly flat surface that minimizes the friction and cutting temperature and produces the better surface finish. This effect is called a mending effect [21]. Also, nanoparticles have a great ability to penetrate into the contact surfaces easily and exhibited significant elasto-hydrodynamic lubrication performance [55]. According to Sahu et al. [38] machining with spray impingement cooling introduced an improved result because in spray cooling, cutting fluid was supplied at high pressure and high velocity, which penetrates through capillary action into the chip-tool interface that causes the reduction of friction as a result cutting temperature reduces and surface quality improved compared with dry condition. Nanofluid has greater wetting as well as lubricating characteristics of the tool tip and as a result, heat dissipation phenomena from cutting zone are improved and favor smoother machining with good quality of surface finish compared with dry [44]. The influence of nanofluid concentration on surface roughness is clearly found in the analysis. For both nanofluids, surface roughness reduces when concentration increases from 0.005 to 0.01% weight % while in a further increase in concentration (0.05 wt%) surface roughness significantly improved. Similar observations were reported by Rahmati et al. [55]. Under nanofluid machining, protective thin films containing billions of nanoparticles were formed on to the finished work surface and enabled much lower friction as well as thermal deformation compared with the un-machined work

surface. This protective film amplified when concentration increases up to a certain limit and beyond it, less protective film produced thus surface quality improved up to a certain limit of concentration and beyond it, the surface quality diminishes. Also, nanoparticles at higher concentrations forcibly impinged by compressed air into pores of the surface. Further, these nanoparticles were sheared off by other incoming nanoparticles and more plowed off particles are remained on to the thin protective film as a result, rougher surface is produced at 0.05 wt% of nanofluid compared with 0.01 and 0.005 wt% [55–56].

In every test run, the shape of the chip is found to be helical in nature. In the current work, as hardness of D2 steel is  $55 \pm 1$  HRC, i.e., it is semi brittle in nature; therefore, helical chips of small segments are produced due to brittle fracture of work-piece during machining. Das et al. also found helical chips at a cutting speed of 100 m/min with feed rate 0.05 mm/rev in hard turning of AISI 4340 steel under dry condition [57]. Also, according to Chandra et al. [58], helical chips produced under non-orthogonal turning which satisfied the current turning condition. Chip helix angle ( $\lambda$ ) is the angle between the chip curl axis and the tangent of the chip curl surface as shown in Fig. 8 [59]. The higher chip helix angle is noticed with nano Al<sub>2</sub>O<sub>3</sub> cutting fluid compared with nano TiO<sub>2</sub> cutting fluid due to the formation of a thicker hydro-dynamic layer between chip and tool [44]. Also, helix angle of chip depends on thermal conductivity of nanofluid; therefore, as thermal conductivity of Al<sub>2</sub>O<sub>3</sub> nanofluid is more than TiO<sub>2</sub> nanofluid, hence,  $\lambda$  is higher for Al<sub>2</sub>O<sub>3</sub> nanofluid. During cutting action, the bottom portion of chips which are in contact with tool-rake surface get expanded due to higher cutting temperature but at the same time, the top portion of chips is adhered with nanofluid; thus, due effective cooling takes place and chips experienced contraction as latent heat of chip is absorbed by nanofluid droplets by evaporative cooling. Therefore, due to this expansion and contraction, chip curling produced [60]. Also, chip curl radius increases with the concentration of nanoparticles in the cutting fluid. It may be due to the higher amount of nanoparticles strike on to the tool rake which accelerates the curliness of chip [44, 58]. Metallic color chips confirm the generation of lower chip-tool interface temperature (Figs. 7 and 8). In every test run, saw-tooth shape has been noticed due to periodically fracture of work material by occurring very high intensity of shear bands during machining [37]. From Fig. 8a–f, it can be stated that the chip segmentation under different nanofluid concentrations is different. In general, segmental chips are produced during machining of hardened steel and this occurrence is directly linked to cutting force fluctuations and stress distribution in the work area and also affects the temperature distribution, and thus the results of the process [61]. Under nanofluid machining, due to increasing concentration of nanofluid, the chip segmental length decreases due to occurrence of more intensity of load on to the

**Fig. 8** Chip micrographs. **a, b** 0.005% weight concentrations. **c, d** 0.01% weight concentration. **e, f** 0.05% weight concentration



formed chip because of the large number of nanoparticle present in the higher concentration of nanofluid. Also, from the thermal conductivity results (Table 1), the thermal conductivity increases with the leading concentration of nanoparticle in the base fluid, which increases the heat transfer rate; thus, rapid quenching of chips takes place. Due to this rapid quenching and continuous impingement of nanofluid, the chip gets segmented in small continuous length chips.

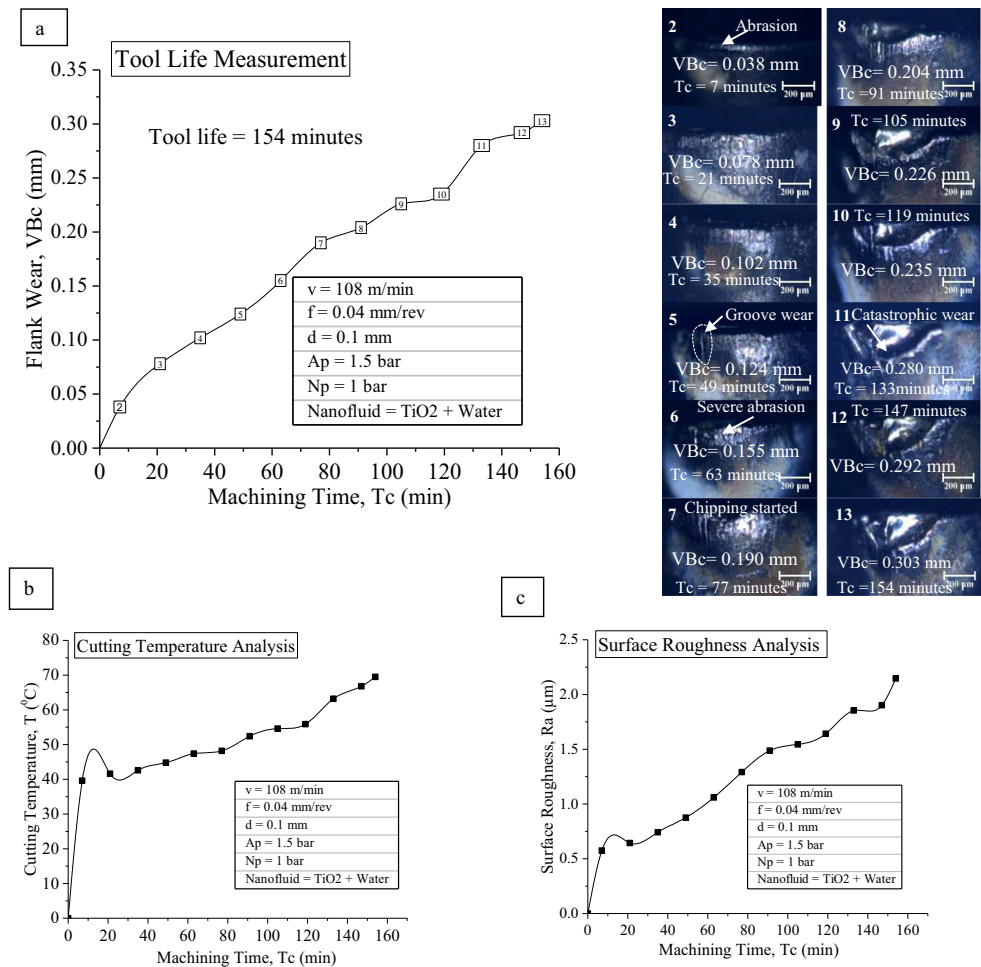
For tool life assessment, nano  $\text{TiO}_2$  cutting fluid with weight concentration of 0.01% has been taken as it provides the best result among all tests considering flank wear criterion of  $\text{VBc} = 0.3 \text{ mm}$  [35–36, 62–64]. The cutting and spraying nanofluid parameters are as follows:  $v = 108 \text{ m/min}$ ;  $f = 0.04 \text{ mm/rev}$ ;  $d = 0.1 \text{ mm}$ ,  $A_p = 1.5 \text{ bar}$ ; and  $N_p = 1 \text{ bar}$  [36]. Flank wear has been assessed with machining time and tool life is noted to be 154 min, Fig. 9a. On similar cutting variables, Kumar et al. found the tool life of 61 min under dry

cutting [35] and 105 min under air-water mist spray cooling environment [36], i.e., with nano  $\text{TiO}_2$  cutting fluid, 2.52 times more tool life is obtained compared with dry cutting and 1.47 times higher tool life obtained compared with air-water mist spray cooling environment due to excellent wettability, lubrication, and heat dissipation capability of nano  $\text{TiO}_2$  cutting fluid during turning.

During tool life evaluation, tool-tip wear gradually improves with the progress of machining time as shown in Fig. 9a. The mechanisms like abrasion, notching, chipping, and catastrophic failure of the tool are major phenomena identified during tool life evaluation [36, 65]. Till 35 min of machining, only the abrasion dominates and is responsible for wear growth as shown in Fig. 9a. Groove wear is noticed after 49 min and continued to 77 min. Chipping phenomena started at 77 min and it continued till 119 min of machining. Further, the chipping phenomena are



**Fig. 9** Evaluation of **a** tool life, **b** cutting temperature, and **c** surface roughness under 0.01% weight concentration of nano TiO<sub>2</sub> cutting fluid



converted into catastrophic failure of tool tip due to high stress and high temperature as shown in Fig. 9a. Further, tool wear width reached to its limit of 0.3 mm at 154 min of machining.

Also higher heat dissipation quality of TiO<sub>2</sub> fluid exhibits a significant reduction in cutting temperature as shown in Fig. 9b. Due to this reduction in cutting temperature, the tool wear growth is also reduced which is confirmed through the tool life result (Fig. 9a). Formation of a hydrodynamic layer on to the tool tip also restricts the heat inside the tool tip thus lowers temperature generation in machining which is confirmed by IR thermal imager where maximum temperature obtained at the end of tool life is 69.5 °C. On same cutting conditions, Kumar et al. [35] found the chip-tool interface temperature at end of tool life under the dry condition of 442.3 °C which is about 6.36 times higher than the temperature obtained under nano-TiO<sub>2</sub> cutting fluid condition. Similarly in another work by Kumar et al. [36], at same cutting condition under air-water mist spray cooling, the cutting temperature at the end of tool life is 160.6 °C, i.e., compared with nano TiO<sub>2</sub> cutting fluid, about 2.31 times more temperature is generated under air-water mist spray cooling. From Fig. 9b, it is clearly noticed

that the growth in temperature is almost steady initially (up to 63 min) and then increasing at the end of tool life.

Surface roughness also improves steadily with the progress of machining time as shown in Fig. 9c due to lower wear rate under nanofluid spray cooling. At surface roughness criteria of 1.6 μm, the tool life was found as about 110 min which is good enough for hard turning concern. At the end of tool life, surface roughness is noticed to be 2.146 μm due to chipping action which results in non-uniform contact between work and tool during cutting.

### 4 Conclusions

Based on the performance of water-based nano-Al<sub>2</sub>O<sub>3</sub> and nano-TiO<sub>2</sub> cutting fluid using spray impingement technique in hard machining, the following conclusions are made:

- High-energy ball mill is utilized to convert micro-sized raw powder of Al<sub>2</sub>O<sub>3</sub> and TiO<sub>2</sub> into nano-sized powder and an average diameter of Al<sub>2</sub>O<sub>3</sub> and TiO<sub>2</sub> are 44 nm and 27 nm, respectively.

- In each % weight of concentration (0.005, 0.01, and 0.05), nano TiO<sub>2</sub> cutting fluid exhibits better results on machinability over nano Al<sub>2</sub>O<sub>3</sub> cutting fluid due to the higher lubricious and wettability characteristics. Also, it may be due to the higher particle size of Al<sub>2</sub>O<sub>3</sub> compared with TiO<sub>2</sub>.
- Most favorable result among all machinability experiments is found at 0.01 wt% concentrations of TiO<sub>2</sub> fluid. At this condition, compared with nano Al<sub>2</sub>O<sub>3</sub> cutting fluid, nano TiO<sub>2</sub> cutting fluid attributed a significant reduction in tool wear (29%), in cutting temperature (9.7%) and in surface roughness (14.3%).
- 29% and 27.7% less tool wear was noticed under nano TiO<sub>2</sub> fluid (0.01% weight) machining compared with dry cutting and air-water-based spray impingement cooling, respectively.
- Abrasion and micro-grooves are identified as the major form of tool wear for both cutting fluids. Higher helix angle and higher curl radius of the chip are noticed under Al<sub>2</sub>O<sub>3</sub> cutting fluid and these parameters are increasing with % weight concentration of both nanofluids. Increasing helix angle may happen due to the formation of a thicker hydro-dynamic layer between chip and tool. Helical and metallic chips are identified in every run with saw-tooth profile due to periodic fracture of work material. Among all set of experiments, lowest cutting temperature obtained under nano TiO<sub>2</sub> cutting fluid (0.01% weight concentration) is with an average value of 39.0 °C which is 77.2%, 68.5%, 9.72% lower than the temperature obtained under dry, air-water mist spray cooling, and Al<sub>2</sub>O<sub>3</sub> nanofluid (0.01% weight concentration), respectively.
- Tool life at 0.01 wt% concentrations of nanoTiO<sub>2</sub> cutting fluids found to be 154 min taking flank wear criteria of 0.3 mm, which is 2.52 times more than the tool life obtained under dry cutting due to excellent wettability, lubrication, and heat dissipation capability. Abrasion, groove wear, and chipping are noticed during tool life assessment. Also, higher heat dissipation quality of TiO<sub>2</sub> fluid lowers the chip-tool interface temperatures which retard the growth of wear and improves surface quality.

In this work, the nozzle position is kept perpendicular to the rake surface. So variations in the nozzle position may influence the machining performance so it may be considered in future work. In mostly published work, only the MQL technique was used for nanofluid cooling, so there is a scope to use spray impingement cooling technique and compared its result with MQL. In the current work, the spray impingement cooling technique with TiO<sub>2</sub> nanofluids (0.01 wt%) outperformed and may be applied in the future for other metal machining processes. Besides, the nanofluid can be prepared using hybrid nanoparticles and may be investigated in applications like machining, heat exchangers, and lubricants under high-pressure circumstances.

**Acknowledgments** The authors are thankful to the Kalinga Institute of Industrial Technology (KIIT), Bhubaneswar, India, for providing the facilities to accomplish the current work.

## References

1. Sharma AK, Tiwari AK, Dixit AR (2015) Progress of nanofluid application in machining: a review. *Mater Manuf Process* 30(7): 813–828
2. Sharma AK, Tiwari AK, Dixit AR (2015) Improved machining performance with nanoparticle enriched cutting fluids under minimum quantity lubrication (MQL) technique: a review. *Mater Today Proc* 2:3545–3551
3. Lee CG, Hwang YJ, Choi YM, Lee JK, Choi COJMA (2009) Study on the tribological characteristics of graphite nano lubricants. *Int J Precis Eng Manuf* 10(1):85–90
4. Sidik NAC, Samion S, Ghaderian J, Yazid MNAWM (2017) Recent progress on the application of nanofluids in minimum quantity lubrication machining: a review. *Int J Heat Mass Transf* 108: 79–89
5. Rapeti P, Pasam VK, Gurram KMR, Revuru RS (2018) Performance evaluation of vegetable oil based nano cutting fluids in machining using grey relational analysis-a step towards sustainable manufacturing. *J Clean Prod* 172:2862–2875
6. Singh RK, Dixit AR, Mandal A, Sharma AK (2017) Emerging application of nanoparticle-enriched cutting fluid in metal removal processes: a review. *J Brazil Soci Mech Sci Eng* 39(11):4677–4717
7. Sharma AK, Tiwari AK, Singh RK, Dixit AR (2016) Tribological investigation of TiO<sub>2</sub> nanoparticle based cutting fluid in machining under minimum quantity lubrication (MQL). *Mater Today Proc* 3: 2155–2162
8. Hegab H, Kishawy HA, Umer U, Mohany A (2019) A model for machining with nano-additives based minimum quantity lubrication. *Int J Adv Manuf Technol*. 102:2013–2028. <https://doi.org/10.1007/s00170-019-03294-0>
9. Sharma AK, Tiwari AK, Dixit AR, Singh RK, Singh M (2018) Novel uses of alumina/graphene hybrid nanoparticle additives for improved tribological properties of lubricant in turning operation. *Tribo Int* 119:99–111
10. Chetan BBC, Ghosh S, Rao PV (2016) Application of nanofluids during minimum quantity lubrication: a case study in turning process. *Tribo Int* 101:234–246
11. Khandekar S, Sankar MR, Agnihotri V, Ramkumar J (2012) Nano-cutting fluid for enhancement of metal cutting performance. *Mater Manuf Process* 27(1–5):963–967
12. Duc TM, Long TT, Ngoc TB (2017) Performance of Al<sub>2</sub>O<sub>3</sub> nanofluids in minimum quantity lubrication in hard milling of 60Si<sub>2</sub>Mn steel using cemented carbide tools. *Adv Mech Eng* 9(7): 1–9
13. Sayuti M, Sarhan AAD, Salem F (2014) Novel uses of SiO<sub>2</sub> nanolubrication system in hard turning process of hardened steel AISI4140 for less tool wear, surface roughness and oil consumption. *J Clean Prod* 67:265–276
14. Garcia GE, Trigos F, Cortes DM, Paras LP (2018) Optimization of surface roughness on slitting knives by titanium dioxide nano particles as an additive in grinding lubricant. *Int J Adv Manuf Technol*. 96:4111–4121
15. Kadrigama K, Anamalai K, Ramachandran K, Ramasamy D, Samykan M, Kottasamy A, Lingenthiran, Rahman MM (2018) Thermal analysis of SUS 304 stainless steel using ethylene glycol/nanocellulose-based nanofluid coolant. *Int J Adv Manuf Technol* 97:2061–2076
16. Najiha MS, Rahman MM, Kadrigama K (2016) Performance of water-based TiO<sub>2</sub> nanofluid during the minimum quantity

- lubrication machining of aluminium alloy AA6061-T6. *J Clean Prod* 135(1):1623–1636
17. Rahman SS, Ashraf MZI, Amin AKMN, Bashar MS, Ashik MFK, Kamruzzaman M (2019) Tuning nanofluids for improved lubrication performance in turning biomedical grade titanium alloy. *J Clean Prod* 206:180–196
  18. Sahu NK, Andhare AB, Raju RA (2018) Evaluation of performance of nanofluid using multiwalled carbon nanotubes for machining of Ti-6AL-4V. *Mach Sci Technol* 22(3):476–492
  19. Raju RK, Andhare A, Sahu NK (2017) Performance of multiwalled carbon nanotube-based nanofluid in turning operation. *Mater Manuf Process* 32(13):1490–1496
  20. Padmini R, Krishna PV, Rao GKM (2016) Effectiveness of vegetable oil based nanofluids as potential cutting fluids in turning AISI 1040 steel. *Tribo Int* 94:490–501
  21. Musavi SH, Davoodi B, Niknam SA (2019) Effects of reinforced nanoparticles with surfactant on surface quality and chip formation morphology in MQL-turning of superalloys. *J Manuf Process* 40:128–139
  22. Amrita M, Srikant RR, Sitaramaraju AV, Prasad MMS, Krishna PV (2013) Experimental investigations on influence of mist cooling using nanofluids on machining parameters in turning AISI 1040 steel. *Proc Inst Mech Eng J* 227:1334–1346
  23. Amrita M, Shariq SA (2014) Experimental investigation on application of emulsifier oil based nano cutting fluids in metal cutting process. *Procedia Eng* 97:115–124
  24. Amrita M, Srikant RR, Raju AVSR (2015) Performance evaluation and economic analysis of minimum quantity lubrication with pressurized/non-pressurized air and nanofluid mixture. *Int J Aero Mech Eng* 9(6):1012–1017
  25. Su Y, Gong L, Li B, Liu Z, Chen D (2016) Performance evaluation of nanofluid MQL with vegetable-based oil and ester oil as base fluids in turning. *Int J Adv Manuf Technol* 83:2083–2089
  26. Duc TM, Long TT, Chien TQ (2019) Performance evaluation of MQL parameters using Al<sub>2</sub>O<sub>3</sub> and MoS<sub>2</sub> nanofluids in hard turning 90CrSi steel. *Lubricants* 7:40
  27. Hegab H, Kishawy HA (2018) Towards sustainable machining of Inconel 718 using nano-fluid minimum quantity lubrication. *J Manuf Mater Process* 2:50
  28. Dong PQ, Duc TM, Long TT (2019) Performance evaluation of MQCL hard milling of SKD 11 tool steel using MoS<sub>2</sub> nanofluid. *Metals* 9:658
  29. Nayak SK, Mishra PC, Parashar SKS (2016) Enhancement of heat transfer by water-Al<sub>2</sub>O<sub>3</sub> and water-TiO<sub>2</sub> nanofluids jet impingement in cooling hot steel surface. *J Exp Nanosci* 11(16):1253–1273
  30. Karimzadehkhoei M, Shojaeian M, Sendur K, Mengüç MP, Kosar A (2017) The effect of nanoparticle type and nanoparticle mass fraction on heat transfer enhancement in pool boiling. *Int J Heat Mass Transf* 109:157–166
  31. Murshed SMS, Leong KC, Yang C (2008) Investigations of thermal conductivity and viscosity of nanofluids. *Int J Therm Sci* 47:560–568
  32. Chiam HW, Azmi WH, Usri NA, Mamat R, Adam NM (2017) Thermal conductivity and viscosity of Al<sub>2</sub>O<sub>3</sub> nanofluids for different based ratio of water and ethylene glycol mixture. *Exp Thermal Fluid Sci* 81:420–429
  33. Yu W, Xie H (2012) A review on nanofluids: preparation, stability mechanisms, and applications. *J Nanomater* 2012:1–17
  34. Mishra PC, Mukherjee S, Nayak SK, Panda A (2014) A brief review on viscosity of nanofluids. *Int Nano Lett* 4:109–120
  35. Kumar R, Sahoo AK, Mishra PC, Das RK (2018) Comparative study on machinability improvement in hard turning using coated and uncoated carbide inserts: part II modeling, multi-response optimization, tool life, and economic aspects. *Adv Manuf* 6(2):155–175
  36. Kumar R, Sahoo AK, Mishra PC, Das RK (2019) Measurement and machinability study under environmentally conscious spray impingement cooling assisted machining. *Measurement* 135:913–927
  37. Kumar R, Sahoo AK, Mishra PC, Das RK, Ukamanal M (2018) Experimental investigation on hard turning using mixed ceramic insert under accelerated cooling environment. *Int J Ind Eng Comput* 9(4):509–522
  38. Sahu SK, Mishra PC, Orta K, Sahoo AK (2015) Performance assessment in hard turning of AISI 1015 steel under spray impingement cooling and dry environment. *Proc Inst Mech Eng J* 229(2):251–265
  39. Kumar R, Sahoo AK, Mishra PC, Das RK (2018) An investigation to study the wear characteristics and comparative performance of cutting inserts during hard turning. *Int J Mach Mach Mater* 20(4):320–344
  40. Saedon JB (2011) Micromilling of hardened (62 HRC) AISI D2 cold work tool steel, Doctor of philosophy thesis. The University of Birmingham UK
  41. Babu MN, Anandan V, Muthukrishnan N, Gajendiran M (2018) Experimental process to evaluate the minimum quantity lubrication technique using copper nanofluids in turning process. *Int J Mach Mach Mater* 20(6):497–512
  42. Duc TM, Long TT, Dong PQ (2019) Effect of the alumina nanofluid concentration on minimum quantity lubrication hard machining for sustainable production. *Proc Inst Mech Eng C J Mech Eng Sci* 233(17):5977–5988
  43. Hegab H, Darrars B, Kishawy HA (2018) Sustainability assessment of machining with nano-cutting fluids. *Proced Manuf* 26:245–254
  44. Hegab H, Umer U, Soliman M, Kishawy HA (2018) Effects of nano-cutting fluids on tool performance and chip morphology during machining Inconel 718. *Int J Adv Manufact Technol* 96(9–12):3449–3458
  45. Khajehzadeh M, Moradpour J, Razfar MR (2019) Influence of nanolubricant particles' size on flank wear in hard turning. *Mater Manuf Process* 34(5):494–501
  46. Chinchalikar S, Choudhury SK (2015) Predictive modeling for flank wear progression of coated carbide tool in turning hardened steel under practical machining conditions. *Int J Adv Manuf Technol* 76:1185–1201
  47. Boothroyd G, Knight WA (2006) *Fundamentals of machining and machine tools*, third edn. CRC Press, Taylor & Francis
  48. Zong WJ, Sun T, Li D, Cheng K, Liang YC (2008) XPS analysis of the groove wearing marks on flank face of diamond tool in nanometric cutting of silicon wafer. *Int J Mach Tools Manuf* 48(15):1678–1687
  49. Sharma AK, Singh RK, Dixit AR, Tiwari AK, Singh M (2019) An investigation on tool flank wear using alumina/MoS<sub>2</sub> hybrid nanofluid in turning operation. *Adv Manuf Eng Mater*:213–219
  50. Xuan Y, Li Q (2000) Heat transfer enhancement of nanofluids. *Int J Heat fluid Transf* 21:58–64
  51. Fathima R, Mujeeb A (2018) Laser induced synthesis and concentration dependent thermo-optical properties of silver-gold alloy nanoparticles. *Mater Res Express* (in press). <https://doi.org/10.1088/2053-1591/aae19c>
  52. Das A, Pradhan O, Patel SK, Das SR, Biswal BB (2019) Performance appraisal of various nanofluids during hard machining of AISI 4340 steel. *J Manuf Proc* 46:248–270
  53. Patole PB, Kulkarni VV (2017) Experimental investigation and optimization of cutting parameters with multi response characteristics in MQL turning of AISI 4340 using nano fluid. *Cogent Eng* 4:1303956
  54. Liew PJ, Shaaroni A, Sidik NAC, Yan J (2017) An overview of current status of cutting fluids and cooling techniques of turning hard steel. *Int J Heat Mass Transf* 114:380–394
  55. Rahmati B, Sarhan AAD, Sayuti M (2014) Morphology of surface generated by end milling AL6061-T6 using molybdenum disulfide

- (MoS<sub>2</sub>) nanolubrication in end milling machining. *J Clean Prod* 66(1):685–691
56. Rapoport L, Nepomnyashchy O, Lapsker I, Verdyan A, Moshkovich A, Feldman Y, Tenne R (2005) Behavior of fullerene-like WS<sub>2</sub> nanoparticles under severe contact conditions. *Wear* 259:703–707
  57. Das SR, Panda A, Dhupal D (2017) Experimental investigation of surface roughness, flank wear, chip morphology and cost estimation during machining of hardened AISI 4340 steel with coated carbide insert. *Mech Adv Mater Mod Proc* 3:9
  58. Chandra A, Pavan K, Adam B, Jie W, Gap-Yong K (2013) Chip segmentation in machining: a study of deformation localization characteristics in Ti6Al4V. *Mechanical Engineering Conference Presentations, Papers, and Proceedings* 89 [https://lib.dr.iastate.edu/me\\_conf/89](https://lib.dr.iastate.edu/me_conf/89)
  59. Rakesh M, Datta S (2019) Effects of cutting speed on Chip characteristics and tool Wear mechanisms during dry machining of Inconel 718 using uncoated WC tool. *Arab J Sci Eng*:1–18
  60. Das A, Patel SK, Das SR (2019) Performance comparison of vegetable oil based nanofluids towards machinability improvement in hard turning of HSLA steel using minimum quantity lubrication. *Mech Ind* 20:506
  61. Neslusan M, Sípek M, Mrazik J (2012) Analysis of chip formation during hard turning through acoustic emission. *Mater Eng* 19:1–11
  62. Nune MMR, Chaganti PK (2019) Development, characterization, and evaluation of novel eco-friendly metal working fluid. *Measurement* 137:401–416
  63. Negrete CC, Najera DC (2019) Sustainable machining as a mean of reducing the environmental impacts related to the energy consumption of the machine tool: a case study of AISI 1045 steel machining. *Int J Adv Manuf Technol* 102(1–4):27–41
  64. Kumar R, Sahoo AK, Mishra PC, Das RK (2018) Comparative investigation towards machinability improvement in hard turning using coated and uncoated carbide inserts: part I experimental investigation. *Adv Manuf* 6(1):52–70
  65. Zheng G, Xu R, Cheng X, Zhao G, Li L, Zhao J (2018) Effect of cutting parameters on wear behavior of coated tool and surface roughness in high-speed turning of 300M. *Measurement* 125:99–108

**Publisher's note** Springer Nature remains neutral with regard to jurisdictional claims in published maps and institutional affiliations.